FULL SIZE MODEL MANUFACTURING AND ADVANCED DESIGN STATUS OF THE SIS100 MAIN MAGNETS *

E. Fischer†, P. Schnizer, GSI, Darmstadt, Germany
A. Akishin, H. Khodzhibagiyan, A. Kovalenko, JINR, Dubna, Russia
R. Kurnyshov, Elektroplant, Protvino, Russia
P. Shcherbakov, IHEP, Protvino, Russia
G. Sikler, W. Walter, BNG, Würzburg, Germany

Abstract

Following an intensive R&D period on short model magnets, GSI launched the production of three full size dipoles and a quadrupole magnet for SIS 100 in 2007 within the framework of the FAIR project. The first straight dipole manufactured at BNG Würzburg was already shipped to GSI and is prepared for testing. The other magnets to be manufactured applying different technological solutions will be completed until the second half of 2008 by JINR Dubna (a straight dipole and a quadrupole) and by BINP Novosibirsk (a curved dipole). We give a brief description of the main construction details and the technological solutions chosen. We will show the critical parameters to be studied on these magnets and their influence on the final design. We will exemplify that on the dipole, whose design was changed recently to provide even more intensive cycles.

INTRODUCTION

The aim of the FAIR project [1] is to provide high intensity primary and secondary beams of ions and antiprotons for experiments in nuclear, atomic and plasma physics. This requires an upgrade of the existing GSI accelerator facility and the construction of a new accelerator complex. It consists of 2 synchrotrons in one tunnel, SIS100 (100 Tm rigidity), SIS300 (300 Tm rigidity), and several storage rings. SIS100 is the most intensively used accelerator considered as "work horse" of the facility. It will accelerate ions and protons at a high repetition rate at about 1 Hz and either sends them to the targets for Radioactive Ion Beam or Antiproton Beam production or to the SIS300 for further acceleration to higher energies. The Collector Ring / Recycled Experimental Storage Ring complex will cool the secondary beams and accumulate the antiprotons. High Energy Storage Ring and New Experimental Storage Ring are the experimental storage rings for antiprotons and ions, respectively. This paper focuses on the fast ramped superconducting dipoles and quadrupoles of the SIS100 synchrotron. The Nuclotron ring of the JINR Dubna[2] was the starting point for our magnet design. In a first R&D step the main operation criteria (AC loss, magnetic field quality and mechanical stability of the coil) had been improved and were experimental tested on mockups and short model magnets [4]. These results have to be scaled to the larger aperture and increased length of the SIS100 main magnets, which is required to realize the challenging beam characteristics. We present a short overview of the different achievements, made during the R&D on the Nuclotron model magnets, the manufacturing status of the actual full size models, estimate their expected operation limits, discuss two design alternatives with enhanced operation performance next to finite element calculations of the cryogenic loads of the first full size magnet already delivered.

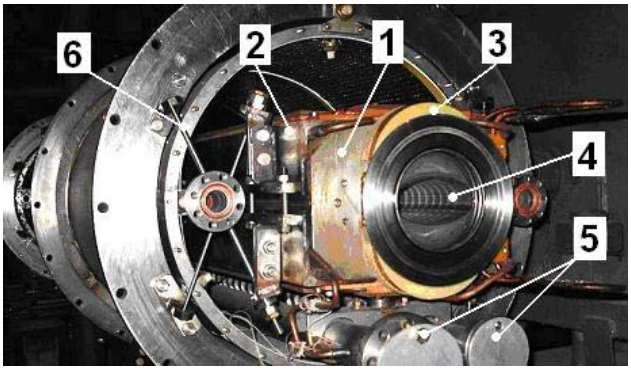

Figure 1: View of the Nuclotron dipole inside cryostat: 1- yoke end plate, 2 brackets, 3 coil end loop, 4 beam pipe, 5 helium headers, 6 suspension

NUCLOTRON MODEL MAGNETS FOR AC LOSS REDUCTION

Dipole

At the original Nuclotron magnets (see figure 1and 2) large AC losses occur during continuously cycling due to eddy currents induced in the cable, in the iron yoke, in the structural elements, (see figure 1 and 2), with 70 % from the cold yoke and 30% from the coil. Further heat is created by the eddy currents in the beam pipe. The yoke losses consist of hysteresis and eddy current losses in the iron and the structural support elements of the magnet. To reduce

* This work is supported by the EU FP6 Design Study (contract 515873 - DIRAC secondary beams) and by the BMBF.
† e.fischer@gsi.de

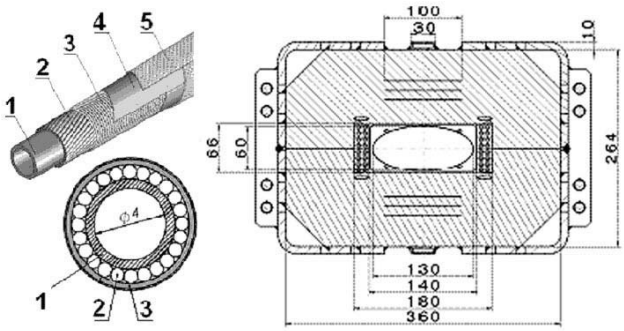

Figure 2: Nuclotron type cable: 1- cooling tube, 2 - Superconducting wire (multifilament NbTi/Cu), 3 - Nichrome wire, 4 - Kapton tape, 5 adhesive Kapton tape. Right: simplified 2D layout of the SIS100 straight dipole with the 2 8 turn two layer coil and the forced flow cooled beam pipe. The six horizontal slits are introduced to suppress the eddy current effects caused by the longitudinal field component near the yokes ends.

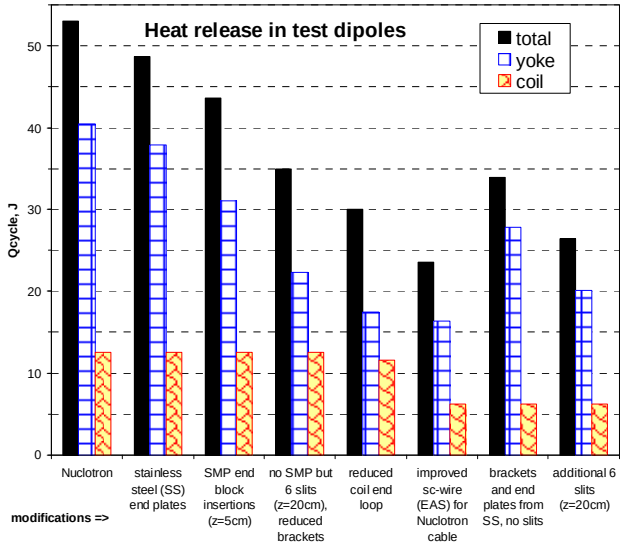

Figure 3: AC losses measured for the different magnet models

.

the load on the cryogenic supply system and thus the operational costs of SIS 100 many single steps were required to obtain a loss reduction[4]. First common sense analysis indicated that the parts made of solid steel (brackets holding the lamination together and the end plates) are the biggest contributors (see figure 3). So the end plates were replaced with stainless steel (SS) ones. Not having reached the set goal the end field was analysed, showing that the component dBz/dz generates losses in the yoke. Following the original idea of the lamination sintered metallic blocks were inserted (SMP) the next step used sheets with slits forming barriers to these currents. The coil ends were modified to fit the beam pipe as closely as possible to reduce the field spreading into the yoke. Cable R&D was carried out

Table 1: Calculated and Measured Dipole Losses

	P_{eddy} [W]	P_{hyst} [W]	[W]	measured [W]
Nuclotron	28.4	16.7	45.1	42 $\pm$2
SS	13.1	9.8	22.9	20

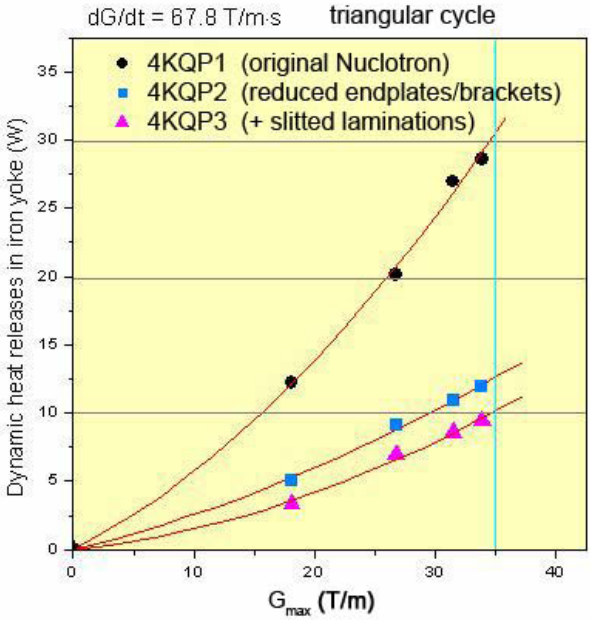

Figure 4: The measured yoke AC loss in a triangular cycle for the different quad- rupoles versus the field gradient at maximum ramp rate

to reduce the losses in the coil; the improved wire ("EAS" wire [5]) with a filament size of 4.1 m was used to fabricate a Nuclotron type cable which reduced the losses even further. In parallel intensive computational studies were conducted. As a result, these losses can be fully calculated by commercial computer programs of today matching the measured values within the measurement precision (see Table 1 [6, 7, 8, 9]).

Quadrupole

Similar improvements were made on the quadrupoles, using the results already obtained in the dipole R&D (see figure 3 [10, 11]). One can see that the maximum loss depends on the maximum gradient. Smaller end plates and slits in the yoke lamination sheets reduced the losses to a third with respect to the Nuclotron magnet.

FULL SIZE MODEL MAGNETS

In the beginning of 2006 the FAIR parameters were actualised within the Baseline Technical Report (FBTR)[12]. According to this status the SIS100 lattice concept had defined the requirements for the straight dipoles and

Table 2: Full Size Modell Magnets

Parameter	Dipole		Quadrupole	
	straight	curved		elongated
maximum field	2.11 T	1.9 T	32 T/m	27 T/m
Magnetic length	2.756 m	3.062 m	1.1 m	1.3 m
Bending angle	3 deg	3 deg	-	-
Curvature radius	47.368 m	52.632 m	-	-
Usable aperture (h·v) mm^2	130·60	115·60	135·65	135·65
Number of magnets	108	108	168	168

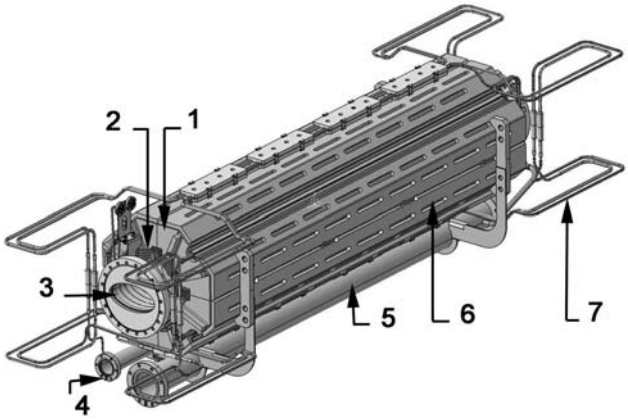

Figure 5: 3D quadrupole model: 1 - end-plate, 2 - coil, 3 - beam pipe, 4 and 5 supply and return helium headers, 6 - brackets fixing the yoke, 7 - bus bars.

quadrupoles as given in Table 2. The following intensive discussion between lattice and magnet designers had shown that an alternative concept using curved dipoles and longer quadrupoles is possible and promising [13]. Table 2 shows the significant reduction of the equivalent horizontal aperture size in the curved dipole due to the eliminated sagitta. The maximum field parameters are substantially reduced too. That offers a more relaxed situation to optimise the field quality. Both these aspects make it possible to reduce the cross section of the laminated yoke as well as the operation current in the coil. This lowers the maximum energy stored in the magnet and also the parasitic AC loss due to eddy currents and hysteresis effect. Besides the cost arguments mentioned above, the minimisation of the total heat loss budget of the dipole is especially important because it limits the possible operation intensity of the synchrotron. The R&D results mentioned above were scaled to the full size magnets in accordance with the SIS100 parameters and had to be verified experimentally. It is also necessary to investigate the technological problems of the intended series production in collaborating with GSI institutes or industry and to gain experience for the magnet tests in the new GSI test facility as well as the methodology of field analysis [14, 15].

Following the decision of the GSI management detailed specifications for the dipole and the quadrupole versions were been worked out. Three collaboration contracts were signed until the end of 2006. The contractors agreed to build two straight dipoles (at JINR Dubna and BNG Wuerzburg), one curved dipole (BINP Novosibirsk) and the elongated Quadrupole (JINR). The tight time scale of the manufacturing processes has been requiring intensive communication and consequent interaction between all the participants. The final design work to prepare the production drawings, the tooling and the technological tests are already completed. The two layer design of the dipole coil is obvious in figure 2. Figure 5 presents the 3D design of the quadrupole chosen for the first full size model. The detailed parameters of this 6 turn per pole option are given

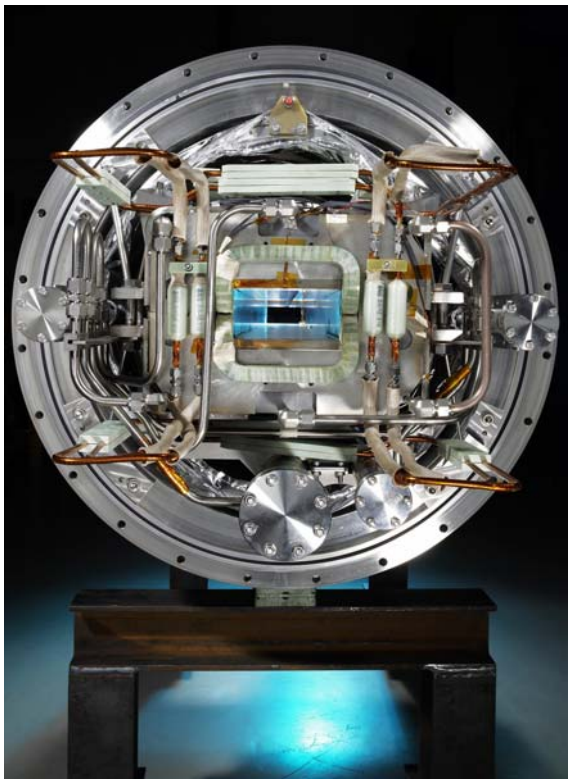

Figure 6: The straight dipole produced by BNG.

in [16]. The required length of the superconducting cable is already produced, i.e. available for all coil winding and the bus bars. The first magnet has already arrived at GSI (see figure 6) and is awaiting its test. The other magnets are expected to follow swiftly during this year [17].

OPERATION CYCLES AND COOLING LIMITS

The practical test of the cooling conditions on the full size models is an important research goal defining the main

Table 3: Operation cycles and expected losses

Cycle	$B_{max}\,[T]$	$t_f\,[s]$	cycle period $[s]$	$Q_d\,[J/cycle]$	$P_d\,[W]$	$Q_q\,[J/cycle]$	$P_q\,[W]$
1	1.2	0.1	1.4	35.2	25.2	13.1	9.4
2a	1.2	0.1	1.4	35.2	25.2	13.1	9.4
2b	0.5	0.1	1.0	8.8	8.8	3.3	3.3
2c	2.0	0.1	1.8	89	48.9	24.4	18.9
3a	1.2	1.3	2.6	35.2	13.5	13.1	5.0
3b	0.5	1.0	1.9	8.8	4.6	3.3	1.8
3c	2.0	1.7	3.4	89	26.2	34.4	10.1
4	2.0	0.1	5.0	89	17.8	34.4	6.9
5	2.0	0.1	5.0	89	17.8	34.4	6.9

operation parameters of the SIS100. The models are based on the hollow Nuclotron cable. Their cooling limits have to be adjusted with the heat loads of the various operation cycles and with the hydraulic resistance of the coil to guaranty a stable two-phase helium flow and a sufficient temperature margin for the superconductor.

Estimation of the Cooling Limits for the Straight dipole

The actual proposed SIS 100 cycles [18] are given for the straight dipole version in Table 3. The injection requires a field of 0.24 T over 0.8 seconds. Then the magnets are ramped up with 4 T/s to the maximum field B_{max}, followed by a flat top time of t_f. The expected dynamic loss per cycle and the average loss power values Q_d, P_d are extrapolated from measurements on short model dipoles. More then 80% of the total AC loss at 4.5 K comes from the iron yoke due to the large cross section. Q_q and P_q are the respective parameters for the quadrupole. Hydraulic calculations had shown that the most intensive cycle 2c should be close to the upper cooling limit [19]. In addition also the low loss limit should be considered in more detail to provide a stable forced flow cooling for all requested operation cycles. These strategic questions will be soon clarified testing the first full size magnet.

Operation test on an equivalent Dipole System

A full length equivalent dipole system was tested to estimate the limits for the cycles. This model dipole consisted of a serial combination of the standard Nuclotron dipole and an optimised short model magnet, both individually tested before. The sum of the AC loss of both 1.4 m long models was close to the total loss expected for the 2.8 m straight dipole. The cooling scheme of the tests is given in figure 7. The coils of the magnets were connected in series with respect to the helium flow and the supply current. For these measurements the cryostat and the power supply system were redesigned at the JINR magnet test facility.

In these measurements the mass flow rate was adjusted for $x_6 \approx 1$, i.e. the mass vapour content at T6 was always close to the critical line of the two-phase helium region.

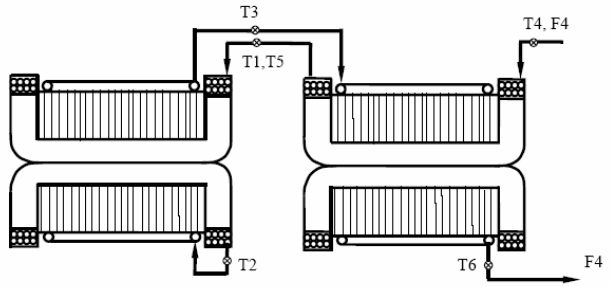

Figure 7: Cooling schema of the equivalent dipole model: T1, T2,...T6 - temperature measurement points, F4 - measured helium flow. The two-phase helium flow enters the laminated yoke after cooling the two short coils all connected in series.

The loss data are in adequate agreement with the values obtained for the individual magnets [20] and confirm our estimations of the cooling limits for the full length dipole. The quench current of the system reached 7916 without preliminary training. The genuine cycle 2c could not be realized, the pause between the ramping had to be increased at least to a cycle period of 2.2s (cycle 2c'). The results are summarised in figure 8. The measured helium pressure drop ΔP dependence on the corresponding time averaged heat loss Q_a in the model dipole is plotted for the cycles given in Table II. A two parameter fit for $\Delta P = c_0 \cdot Q_a^n$ defines $n = 1.733$ and c_0. The parameter $n = 1.75$ is the well know mass flow rate exponent describing the pressure rise due to friction, so $c_0 = 0.00153$ is the only adjusted coefficient. The results for cycle 2c' had shown, that under the given cooling conditions and ramp rates the upper limit for stable cycle operation is defined by $Q_{aL+} = 35\,W$. Using this characteristic value and introducing the maximum pressure drop ΔP_0 we obtain $\Delta P = \Delta P0(Q_a/Q_{aL+})^{1.75}$ with $\Delta P_0 = 0.77$ bar, the microscopic description of these parameters is given in detail in [21]. For the stable cycle 2b (ΔP = 0.15 bar) and the unstable cycle 3b (ΔP =0.10 bar) the loss values could not been measured and was calculated using the fit line. The experimentally obtained stability limit was closer to cycle 3b so we can estimate it as

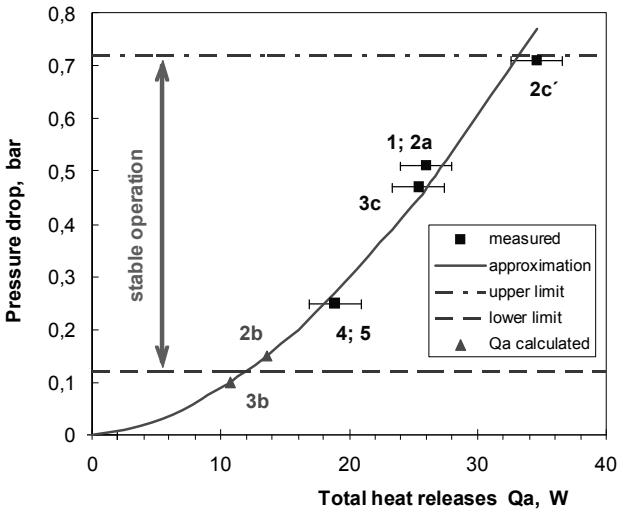

Figure 8: Cryogenic stability range of the 2.8 m long equivalent model dipole. The cycle names are plotted near their data points.

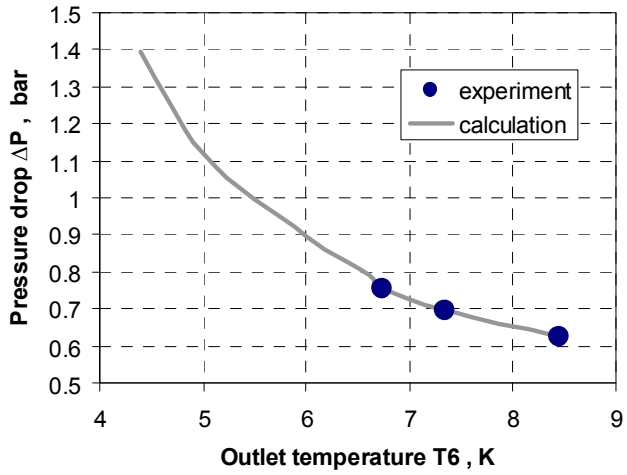

Figure 9: The pressure drop dependence on the yoke outlet temperature at the equivalent model dipole tested and calculated for a stable triangular cycle with the total heat load of 50.5 W.

$P_{min} = 0.12$ bar or $Q_{aL-} = 12W \approx 1/3 Q_{aL+}$.

More intensive cycles require to increase Q_{L+}. This can be achieved by changing the yoke outlet temperature T6 into the vapour area, but assuring $x_2 < 1$ at the outlet of the coil. The method is demonstrated in figure 9 showing the results obtained for the composite dipole, tested this way in a stable triangular cycle with a heat load of 50.5 W, i.e. 50QL+ . In this operation mode the pressure drop spread is reduced by a factor of two (the higher values are calculated). For a cooling scenario with T6=4.4 K (x6=1) we have P = 1.39 bar, i.e. an impossible mode, but the high load cycle was demonstrated with P=0.627 bar choosing T6=8.45K. The same ideas could be applied to extend the SIS100 magnets operation to higher intensities, i.e. for continuous triangular cycles, not shrinking the main cycle limits defined in figure 8. This means, that the magnet design should be optimised for cycle 2c, the more intensive cycles can be provided as shown in this section. Based on a final decision for the main magnet parameters and for the complete required cycle spectra, the magnet design and the cooling modes should be analysed carefully. The optimal operation scenario will be chosen to provide an energy efficient operation of the SIS100.

FINAL DESIGN FOR EXTENDED PERFORMANCE

The performance analysis for the straight model has to be compared with the parameters of the curved dipole. In addition a single layer magnet design was considered given that it provides a much higher cooling power due to the reduced hydraulic resistivity of the coil [20, 22, 23, 24].

Magnetic field of a single layer dipole

A magnet design with the minimal required magnet aperture allows also to reduce the required yoke size and was thus favoured in the beginning. A magnet design was made [25] and the field deterioration analysed. For that circular multipoles of the type

$$\mathbf{B}(\mathbf{z}) = B_0 \sum_{n=1}^{\infty} \mathbf{c_n} \left(\frac{\mathbf{z}}{R_{Ref}} \right)^{n-1} \qquad (1)$$

were used, with the Cartesian coordinates $\mathbf{z} = x + iy$, the magnetic field $\mathbf{B} = B_y + iB_x$ the reference radius R_{Ref} and the relative circular multipoles $\mathbf{c_n}$. These multipoles were obtained by calculated elliptic multipoles and then recalculating them to the circular multipoles using analytical transformations[15, 26], which produces multipoles representing the field within the whole aperture with good accuracy. The relative sextupole b_3 and dekapole b_5 are presented in Fig 10. One can clearly see that the sextupole of the "minimal design" is much bigger at even medium fields than for the double layer version. Thus the free aperture between the coils was increased from 130 to 140 mm (option "CSLD"). One can see that this option provides a sextupole comparable to the curved double layer dipole. The dekapole is even smaller than the one of the curved double layer dipole.

Cooling

Along with the curved single layer dipole a two layer dipole alterantive (C2LD-a) was considered to ensure stable operation modes up to the triangular cycle. The CSLD version is based on our previous R&D on high current Nuclotron type cables experimentally tested in short model dipoles equipped with 8 turn single layer coils [27, 28]. The results had to be adjusted to the parameters and requirements of SIS100 [23]. Besides the CSLD design some other versions and a 10 turn coil were considered too, but

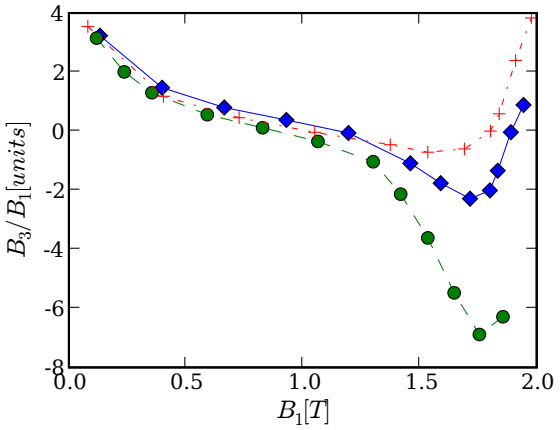

(a) sextupole

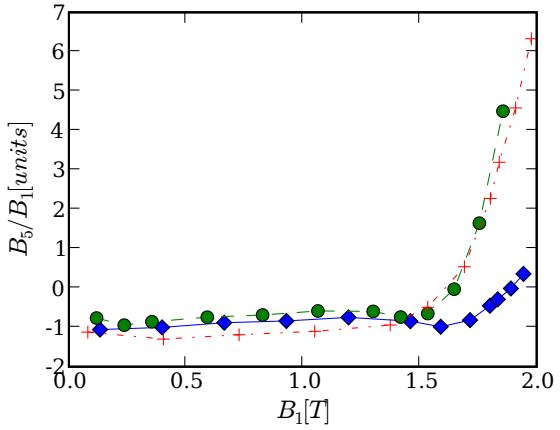

(b) dekapole

Figure 10: The relative strength of the sextupole and octupole (in units) versus the dipole field strength (in Tesla). One unit equals 100 ppm. The blue solid line represents the data for the CSLD, the green dashed line for the design with the minimal aperture and the red dashed dotted line for the curved double layer design.

Table 4: SIS 100 Dipole Options

Parameter Version	straight	curved	C2LD-a	CSLD
Maximum field, T	2.11	1.9	1.9	1.9
Magnetic length, Tm	2.756	3.062	3.062	3.062
Turns per coil	16	16	16	8
Usable aperture, mm2	130 · 60	115 · 60	115 · 60	140 · 60
Cables				
Number of strands	31	31	38	23
Outer diameter, mm	7.36	7.36	7.5	8.25
Cooling tube inner diameter, mm	4	4	4.7	4.7
Length of the cable in the coil, m	110	110	110	57
Bus bars length, m	37	39	39	39
Operating current	7163	6500	6500	13000
Critical current @ 2.1 T, 4.7 K	11900	11900	11900	19840
Wires				
Strand diameter, mm	0.5	0.5	0,46	0.8
Filament diameter, μm	2.5 - 4	2.5 - 4	2.5 - 4	3.5 - 4
Filament twist pitch, mm	45	4-5	4-5	5-8
loss and hydraulic				
Static heat flow, W	7	7	7	7
Heat load to bus bars, W	0.5	0.5	0.5	0.5
cycle 2c				
AC losses, W	36.3	35.4	35.4	35.7
Pressure drop, bar	1.10	1.15	0.604	0.389
T_{max} of He in the coil (for $x_6 \approx 1$) , K	4.94	4.95	4.78	4.64
triangular cycle [dB/dt = 4 T/s, tcycle = 2Bmax / (dB/dt)]				
AC losses, W	75.1	74.0	74.0	74.6
Pressure drop, bar	1.14	1.20	0.657	0.486
T_{max} of He in the coil, K	5.08	5.10	4.86	4.72
with T_6 at	$8K$	$8K$	$8K$	$7K$

detailed field calculations, loss estimations and stability analyses had shown that the CSLD option is clearly the most appropriate alternative [25]. The main design and estimated operation parameters of the actual manufactured full size models and the two alternative options are summarised in Table 4.

For the hydraulic calculations as in [21] the following effects were considered: 1.) Dynamic heat load to the inner layer: 75% of the coil AC loss. 2.) Dynamic heat load to the outer layer: 25% of the total coil AC loss, and 25% of the yoke AC loss. 3.) Dynamic heat load to yoke cooling channel: 75% of the yoke AC loss. The heat load generated by the vacuum chamber, touching the coil, is not even considered here. The lower part of Table 4 shows, that:

1. The actual manufactured full size dipoles (straight and curved) should operate at their physical limit to provide the most intensive triangular cycle and will not be stable.

2. This problem was identified and thus the CSLD was chosen as design for the SIS 100 main dipole [29] as it can provide the requested triangular cycles as well as a safety cooling margin for additional, not yet identified, heat loads.

THERMAL ANALYSIS USING ANSYS

A real accelerator magnet uses different materials for different parts. The field in the iron and in the aperture is influenced by the 3D geometry of the yoke and the beam pipe structure as well as by the steel B H curves which are

nonlinear and anisotropic, as the yoke is laminated. During an intensive R&D the Nuclotron dipole and quadrupole model magnets were modelled with all their details in ANSYS and it was shown that the AC losses can be calculated agreeing well with the measurements [9]. Based on this knowledge analogous calculations of eddy current and hysteresis losses were conducted for the actual design of the full length SIS100 dipole as built by BNG. Using the results of the electromagnetic field calculations, the analysis is extended to investigate the thermal effects in the main construction elements of the magnet and to estimate the temperature margins of the superconductor and of the cryo-pump functionality of the beam pipe [30].

The superconducting dipole

The straight dipole manufactured by BNG features a yoke, made of laminated electrical steel (1 mm thick), and brackets and end plates of stainless steel. The two layers of its coil are embedded in a G11 matrix. The vacuum chamber structure consists of an elliptical beam pipe (inner aperture: 130 mm 60 mm, 0.3m thick stainless steel), cooling tubes and the mechanical stabilising transversal ribs (1 mm thickness, 20 mm transposition pitch). The thermal contact between vacuum chamber, coil and yoke is provided by electrically insulating G11 plates. The specific problems of finite element simulations for the real geometry of fast ramping superferric magnets, consisting of various ferromagnetic and non magnetic steels with a sophisticated 3D geometry, have been solved with ANSYS using edge elements. To construct an appropriate electromagnetic-thermal 3D model for the new SIS100 full size dipoles and for a correct FE analysis, the design details and material properties of the vacuum chamber are very important, as well as its connection to the coil and the yoke. The middle of the magnet is basically uniform in z, except for the rib structure of the vacuum pipe. Thus a magnet model with a length equal to the period of the rib structure was formed to reduce the number of elements. This requires choosing correct boundary conditions, in particular enforcing eddy current traces always perpendicular to the cross section of our model. The 3D magnetic and the thermal models of magnet centre, equal to one period of the vacuum chamber with ribs, are shown in figures 11 and 12.

The triangular cycle, continuously ramping with 4T/s between the injection field $B_{min}0.24\,T$ and $B_{max} = 2.1T$, is actually the most demanding operation mode for the SIS 100 dipoles [24]. For the analysis the approximation $B_{min} = 0T$ was used as well as a fixed current ramp $|dI/dt| = const$ with a cycle repetition rate of 1Hz. The thermal calculations are done using the time averaged power of the AC loss. The inaccuracy of the so calculated results was estimated to be less then the uncertainties caused by the variation of the material data, i.e., $dB(I)/dt$ is especially sensitive to the material properties B(H) and the real packing factor of the yoke. Following the method given here, the exact calculation will be straight forward

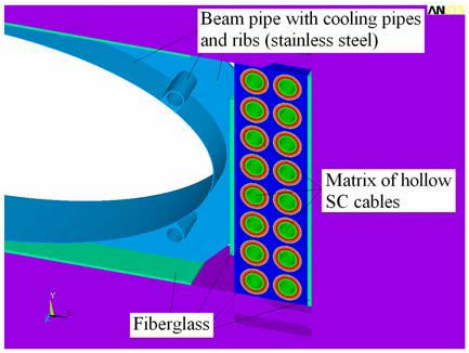

Figure 11: Layout of the main parts of the SIS100 dipole FE model.

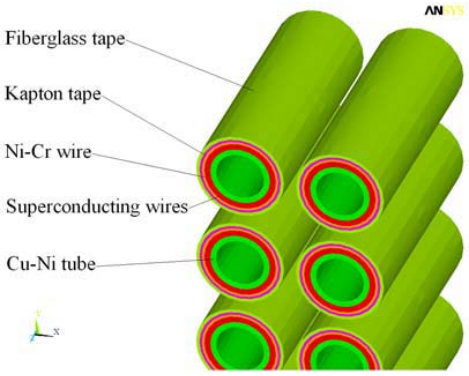

Figure 12: Layout of the turns of the SC coil of the SIS100 dipole magnet.

for all required cycles and all different magnet sizes.

AC Loss Results

The heat sources for the thermal calculations are the magnetic hysteresis and the eddy current loss in the structures of the yoke, the SC coil and the vacuum chamber. The hysteresis loss per cycle is not frequency dependent and can be determined in the static magnetic mode. The eddy current loss was calculated as a transient process. The specific data and methods given in [31, 32] were used for calculating the hysteresis loss in the laminated yoke and in the superconducting multifilamentary wires. The applied electrical resistivities of the conductive materials at 4.2 K are provided in Table 5. The AC loss was integrated over all elements to obtain the contribution of each design unit of the magnet. The main loss sources are summarised in Table 6. The coil loss data are strongly dependent on the SC wire design. The upper extremes of the loss values for

Table 5: Resistivity of materials at 4.2 K $10^{-7}\Omega m$

Electrical steel	Stainless steel	Copper	CuNi	NiCr
3.2	5	0.017	1.4	12

Table 6: Loss per cycle in the different parts of the magnet

	Yoke assembly		Vacuum chamber		SC coil	
	Yoke Hysteresis	Yoke Eddy Currents	Elliptical tube	Cooling pipes	Hysteresis in filaments	Eddy in matrix
AC loss, [J/m]	9.63	0.34	5.18	4.83	2.03-4.1	3.13-6.3
Total	10.05		10.1		5.18-10.4	

the SC coil are given for the wires already tested with a filament diameter of 6 m, the lower values are estimated for wires with 2.5 m filaments. The total values include also the eddy losses in the brackets (0.076 W/m) and the yoke cooling pipe (0.0067 W/m). The loss in the ribs of the vacuum chamber (0.097 W/m) is also negligible as well as the value obtained for the CuNi tubes of the cable (0.021 W/m). To estimate the total thermal loss of the dipole, to be cooled at 4 K, one also has to consider the end field effects ($\approx$ 5 W/dipole) and the static heat load.

Impact on temperature

All thermal contacts between the different electrical conducting or insulating materials of the dipole construction, including the fine structure of the SC cable had been modelled thoroughly. The temperature boundary conditions are chosen to be T = 4.5 K at all inner surfaces of the cooling tubes; the heat flow from surfaces in contact with vacuum was approximated to be zero. The temperature dependence is considered for the thermal properties of all materials (thermal conductivity and specific heat capacity). Some characteristic values of the thermal conductivity and the specific heat capacity at 4.2 K are given in Table 7. The thermal analysis can be carried out in transient or steady state mode, but most of the analysis was performed in steady state mode due to the stable cycle repetition frequency of 1 Hz. The transient calculations, using the time-averaged loss power density, had shown that the steady state is achieved after approximately 60 cycles. The time averaged AC power loss density function was applied to the thermal model and the steady state thermal problem was solved. To check the cryo-pump functionality of the beam pipe, the 3D distributions of the temperature was analysed for different versions of the vacuum chamber construction: (I) for the complete chamber assembly, (II) with the ribs, but without cooling pipes, and (III) the beam pipe with cooling tubes but without ribs (see figure 13) as well as the transversal temperature profiles of the beam pipe in the plane of the rib starting from the small half axis to the large half axis. The maximum temperatures are 11.5 K 13 K and 24.1 K for version I, II and III respectively. The corresponding values between the ribs are 15.3 K, 17.3 K and 24.1 K. This small difference of the data for version I and II suggests, that the thermal contact of the vacuum chamber to the coil and the yoke cools the beam pipe more efficiently than the given cooling tube arrangement. This result is also important for the heat flow balance between the iron yoke and the coil. That finally defines the operation temperatures of the superconducting cable and its temperature margin. The temperature distribution in the superconducting wires, modelled by a cylindrical layer in the hollow superconducting cable, is presented in figure 14 for the two different versions I and III. The CuNi tubes are not shown. It has been obtained from these calculations, that the temperature gradient between the SC wires layer, contacting the outer surface of the CuNi tube, and the inner site of this tube, contacting the flowing helium at 4.5 K, is in the order of 0.01-0.03 K. Taking into account the additional temperature drop between the CuNi cooling tube and the two-phase helium flow as well as the complicated fine structure of the contact surface of the 31 superconducting wires the experimental values should be slightly higher. A maximum temperature difference of 0.2 K was measured in special experiments on Nuclotron dipoles[33]. This shows that the temperature margin of the SC wire is defined by the temperature profile of the two phase helium flow depending on the operation modes.

CONCLUSION

- The main R&D goals for the SIS100 magnets have been reached and were used to specify the design of the first full length model magnets for industrial production.
- The first full size dipole is ready for testing at GSI, a second dipole, a quadrupole and a curved dipole will be ready in third quarter of 2008.
- The comprehensive test of these models will give us important information required to optimise the final design and to specify the pre-series magnets.
- The redesign toward an optimised curved dipole with a single layer coil can fulfil the recently updated operation requirements of the FAIR SIS100 accelerator.
- The ramping fields introduce eddy currents in the current vacuum chamber assembly, which create a significant additional heat load on the superconductor.

ACKNOWLEDGMENT

The authors thank all those who contributed to this work, especially all people from the participating laboratories; in particular from GSI, IHEP, JINR, BNG, BINP and FZK.

Table 7: Thermal conductivity λ and specific heat C of materials at 4.2 K

	Electrical steel	Stainless steel	Copper	CuNi	G11	Kapton
λ W/(mK)	0.8	0.21	630	1.30	0.08	0.012
C, J/(kgK)	0.4	2.1	0.1	0.11	1.55	0.8

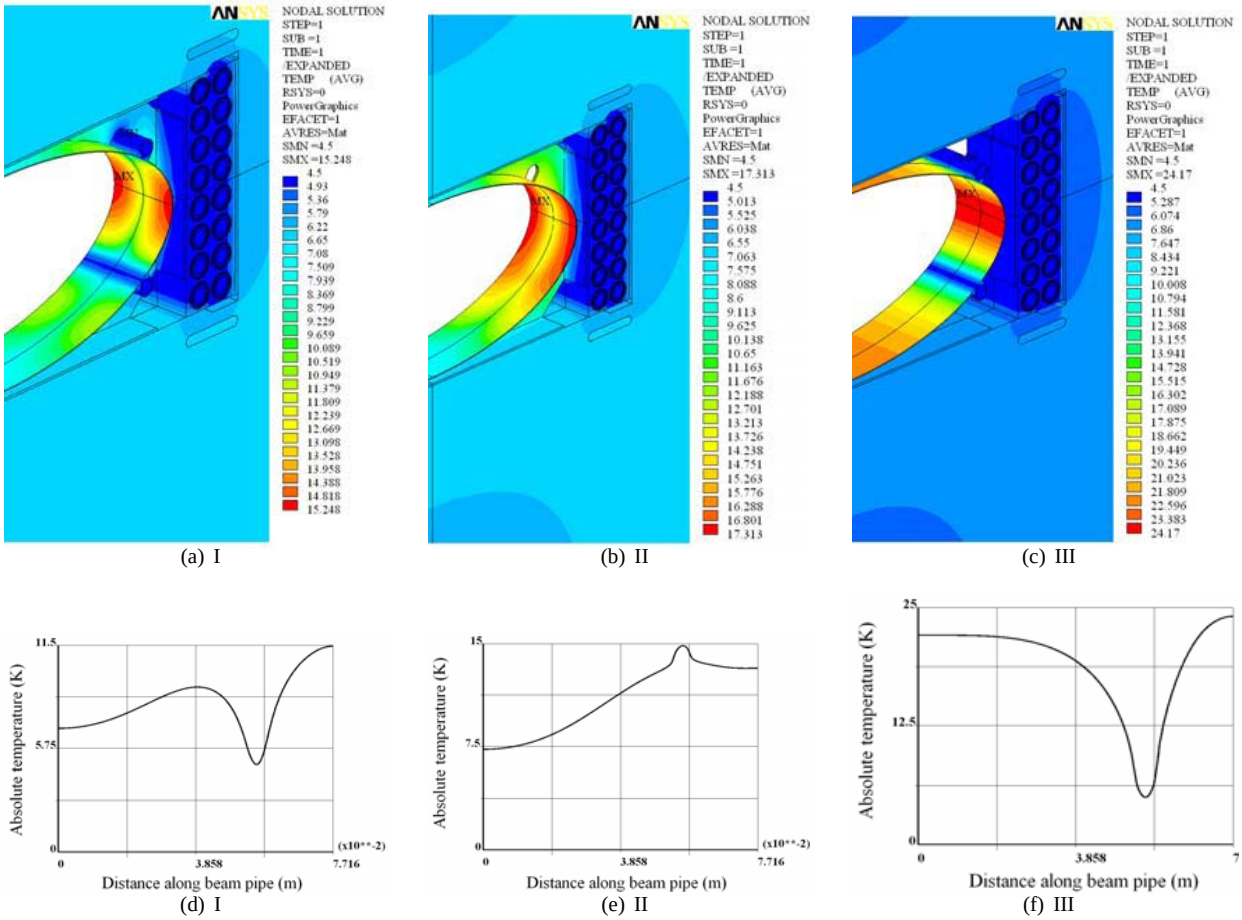

(a) I (b) II (c) III

(d) I (e) II (f) III

Figure 13: Temperature field on the vacuum chamber

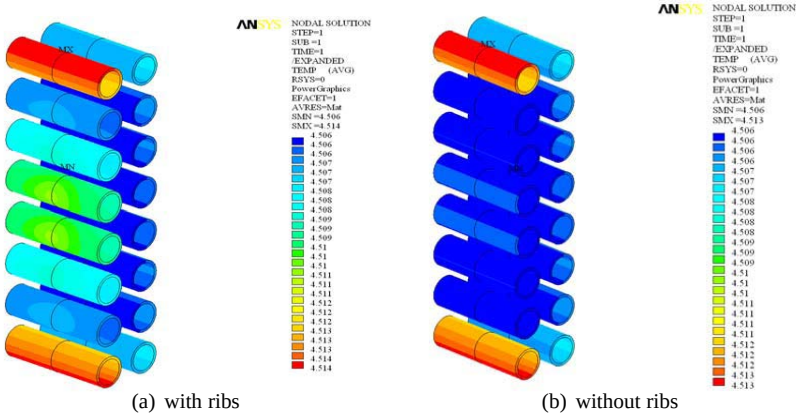

(a) with ribs (b) without ribs

Figure 14: Temperature field in the SC wires of the coil turns.The CuNi tubes, on which the wires are placed, are not shown.

REFERENCES

[1] An International Accelerator Facility for Beams of Ions and Antiprotons. Conceptual Design Report, (2001), http://www.gsi.de/Future/

[2] H.G. Khodzhibagiyan, A.A. Smirnov "The concept of a superconducting magnet system for the Nuclotron", Proc. of the Twelfth Int. Cryogen. Eng. Conf., ICIC12, Southampton, 1988, pp.841-844.

[3] G. Moritz et al., "Towards fast pulsed superconducting synchrotron magnets," in Proc. PAC'2001, Chicago, June 2001, pp. 211-214.

[4] Alexander Kovalenko et.al., "New Results on Minimizing AC Power Losses in a Fast Cycling 2T Superferric Dipole with a Cold Yoke", IEEE Trans. Appl. Supercond., vol. 16, N2, 2006, pp.338-341

[5] "European advanced superconductor," http://www.advancedsupercon.com.

[6] P. Shcherbakov. et .al "3D field computations for the mai prototype magnets of the SIS 100 accelerator of the FAIR Project", Proceedings of EPAC 2006, Edinburgh, June 2006

[7] E. Fischer. et .al "Analysis of the superferric quadrupol magnet design for the SIS 100 accelerator of the FAIR project", Proceedings of EPAC 2006, Edinburgh, June 2006

[8] P. Shcherbakov. et .al "3D Magnetic field and eddy cur rent loss calculations for iron dominated accelerator mag nets using ANSYS compared with results of non commer cial codes", Proceedings of EPAC 2006, Edinburgh, Jun 2006

[9] E. Fischer, R. Kurnyshov and P. Shcherbakov, "Finite element calculations on detailed 3D models for the superferric main magnets of the FAIR SIS100 synchrotron" Cryogenics, (47) 2007, pp 583-594

[10] "Report on research and development contract No 6 between GSI and JINR Dubna", March 2006

[11] EU FP6 'DIRAC secondary Beams', 1st Annual Report, Annex 3: Design report on structural analysis (Deliverable 53 of task 22)

[12] FAIR Baseline Technical Report, GSI, Darmstadt Germany, 2006

[13] E. Fischer, H. Khodzhibagiyan, A. Kovalenko "SIS100: Magnet Design options to minimize the Energy losses, Investment and Operation Costs", MT-INT-EF-2006-002, GSI, 08, 2006

[14] A. Stafiniak et al "Commissioning of the Prototype Test Facility for Rapidly-Cycling Superconducting Magnets for FAIR", IEEE Trans. Appl. Supercon, vol. 18 (2), 2008, pp1625-1628

[15] P. Schnizer, B. Schnizer, P. Akishin, E. Fischer " Magnetic field analysis for superferric accelerator magnets using elliptic multipoles and its advantages", IEEE Trans. Appl. Supercon, vol. 18 (2), 2008, pp1648-1651

[16] E. Fischer, A. Alfeev, A. Kalimov , H. Khodzhibagiyan, A. Kovalenko, G. Kuznetsov, G. Moritz, C. Muehle, and V. Seleznev "Status of the Design of a Full Length Superferric Dipole and Quadrupole Magnets for the FAIR SIS 100 Synchrotron", IEEE Trans. Appl. Supercond., vol. 17, N2, 2007, pp.1078-1082.

[17] A.Kovalenko et. al "Full Size Magnets for Heavy Ion Superconducting Synchrotron SIS100 at GSI: Status of Manufacturingand Test at JINR", 11^{th} European Particle Accelerator Conference, June, 2008, Genova

[18] P. Schuett, "Operation modes of the new accelerator complex for ions and antiprotons", Report on EMAC II, GSI, Darmstadt, October 2003.

[19] E. Fischer, H. Khodzhibagiyan, A. Kovalenko "SIS 100 dipole cooling limits ", MT-INT-EF-2007-002, GSI, 20.05.2007

[20] E. Fischer "FAIR: SIS 100 Synchrotron R&D Status Main Magnets and Full Length Models", miniTAC sc Magnets and Cryogenics, May 24/25 2007, Egelsbach

[21] H. Khodzhibagiyan, A. Kovalenko, and E. Fischer "Some aspects of cable design for fast cycling superconducting synchrotron magnets", IEEE Trans. Appl. Supercond., vol. 14, N2, 2004, pp.1031-1034.

[22] E.Fischer et al., "Minimization of AC Power Losses in Fast Cycling Window Frame 2T Superferric Magnets with the Yoke at T=4.5K", presented at ASC 2004; Internal GSI Note, MT-INT-EF-2004-09

[23] E. Fischer, H. Khodzhibagiyan "SIS 100 dipole alternatives", MT-INT- EF-2007-003, GSI, 15.06.2007

[24] E. Fischer, H. Khodzhibagiyan and A. Kovalenko, IEEE Trans. Appl. Supercon., June, (18) 2008, p 260-263

[25] P. Akishin, E. Fischer, P. Schnizer "A single layer dipole for SIS 100" Gesellschaft für Schwerionenforschung mbH, Tech. Rep., July 2007.

[26] P. Schnizer, B. Schnizer, P. Akishin, E. Fischer "Theoretical Field Analysis for Superferric Accelerator Magnets Using Plane Elliptic or Toroidal Multipoles and its Advantages", 11^{th} European Particle Accelerator Conference, June, 2008, Genova

[27] Khodzhibagiyan, H. E. Fischer, A. Kovalenko, G. Moritz, L. Potanina, A. Shikov, G. Vedernikov "Design and test of a hollow superconducting cable based on keystoned NbTi composite wire", IEEE Trans. Appl. Supercond. (2005) 15 2 1529-1532

[28] H. Khodzhibagiyan, N. Agapov, A. Kovalenko, A. Smirnov, A. Starikov "Development of fast-cycling superconducting magnets at JINR", CRYOPrague 06, Prague, July 2006.

[29] An International Accelerator Facility for Beams of Ions and Antiprotons. Technical Design Report, Synchrotron SIS 100, to be published

[30] E. Fischer, R. Kurnyshov, and P. Shcherbakov, "Analysis of coupled electromagnetic-thermal effects in superconducting accelerator magnets", J. Phys.: Conf. Ser. 97 (2008) 012261 (6pp)

[31] P. Shcherbakov et al. 2004 Magnetic properties of silicon electrical steels and its applications in fast cycling SC magnets at low temperatures, (RUPAC-2004, Dubna) pp 298-300

[32] Superconducting Material Database, article 5. Thermal, Electrical and Mechanical Properties of Materials at Cryogenic Temperatures N 11 FDR 42 01-07-05 R 0.1

[33] H. Khodzhibagiyan et al. "Design of new hollow superconducting NbTi cables for fast cycling synchrotron magnets", IEEE Trans.Appl.Supercond. 2003, 13, N2, pp.3370-3373.